Digest Journal of Nanomaterials and Biostructures Vol. 13, No. 3, July - September 2018, p. 653 - 659

PLASMONIC MATERIAL BASED ON SILVER COLLOID AND Zn-METALLOPORPHYRIN FOR DRUG DETECTION OF *p*-AMINOSALICYLIC ACID

L. SALAGEANU[a], A. LASCU[b], M. BIRDEANU[c], E. FAGADAR-COSMA[b,*]
[a]*Health Insurance House Timis, Corbului Street 4, 300239-Timisoara, Romania*
[b]*Institute of Chemistry Timisoara of Romanian Academy, M. Viteazul Ave. 24, 300223-Timisoara, Romania*
[c]*National Institute for Research and Development in Electrochemistry and Condensed Matter, 1 Plautius Andronescu Street, 300224 Timisoara, Romania*

Para-aminosalicylic acid is still widely used for the efficient treatment of tuberculosis although it is known to cause severe adverse side-effects to the human body. This work presents a simple and efficient spectrophotometric method for PAS detection in the concentration range of medical relevance useful both for pharmaceutical and for medical control. The UV-vis investigations were focused on a comparison of sensing activity of PAS using solely silver nanoparticles or 5,10,15,20-tetrakis-(4-aminophenyl)-porphyrin-Zn(II) or the hybrid material generated between them. The best and accurate detection results of PAS, in the medical relevance window (0.1-30μg/mL), were obtained by using the hybrid material.

(Received May 9, 2018; Accepted July 16, 2018)

Keywords: Silver colloid, Zn-metalloporphyrin, P-aminosalicylic acid detection, AFM, UV-vis spectroscopy

1. Introduction

Although *para*-aminosalicylic acid (PAS) was widely used starting in the 1940s for the treatment of tuberculosis (TB), due to the discovery of antibiotics such as rifampicin and pyrazinamide its prescription was significantly diminished [1].

Although PAS is known to cause several adverse gastrointestinal side-effects (anorexia, diarrhea, nausea, and vomiting) and hypothyroidism, it was reintroduced in 1992 by the United States of America in cases of multi-drug resistant TB. Therefore, it is currently used only by controlled formulations and targeted release [2, 3].

Taking into consideration the drawbacks of PAS intake for TB appropriate treatment, the control of the doses is of major importance to achieve an effective serum concentration [4, 5].

Adequate p-aminosalicylic acid plasma concentrations vary in the range 0.1 micrograms /mL for C_{min} and 8.4 micrograms /mL for C_{max} plasma concentration [6].

The detection of PAS in urine is necessary because, in the case of multi-drug TB treatment, some patients avoid the intake of PAS due to its kidney side effects [7].

Capillary zone electrophoresis was used for the determination of both *p*-aminosalicylic acid (PAS) and its N-acetyl metabolite in urine needing no sample pretreatment [8].

An ion-pairing HPLC method, based on Chromolith Speedrod RP-18e column allowed for simultaneous determination of both *p*-aminosalicylic acid (PAS) and its degradation *m*-aminophenol product [9].

Quantitative determinations of PAS both in pharmaceutical formulations [10, 11] and in biological samples [12, 13] were attempted during time using UV-vis spectrophotometry, fluorescence methods and HPLC.

*Corresponding author: efagadar@yahoo.com

Improving the tuberculosis chemotherapy so that side-effects are reduced is an actual target. The purpose of our work was to provide a simple and efficient spectrophotometric method for PAS detection in the concentration range of medical relevance (2 μg/mL-30 μg/mL) useful both for pharmaceutical and for medical control.

Based on our previous experience in using plasmonic silver or gold colloids and diverse porphyrin derivatives to detect biologically active or pharmaceutical compounds [14-17], this work is based on a complex between silver nanoparticles (*AgNPs*) [18, 19] and 5,10,15,20-tetrakis-(4-aminophenyl)-porphyrin-Zn(II) (*ZnTAPP*), with structure depicted in Figure 1, sensitive to PAS monitoring by simple UV-vis spectroscopy. *AgNPs* were chosen owing to their excellent enhancing absorption properties and the Zn-amino substituted porphyrin due to the proven capacity of the Zn porphyrins to detect organic compounds containing amino-groups [20].

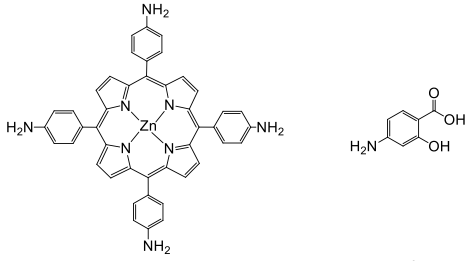

1 **2**

Fig. 1. Structures of: 5,10,15,20-tetrakis-(4-aminophenyl)-porphyrin-Zn(II)(1) and of 4-aminosalicylic acid (2).

2. Experimental

2.1. Reagents

The reagents used in this work have been provided by Sigma-Aldrich and Merck and were *purum analiticum* grade. Silver nanoparticles were obtained by a previously reported method [21]. The 5,10,15,20-tetrakis-(4-aminophenyl)-porphyrin-Zn(II) was provided by Por-Lab GmbH (Germany). The hybrid between porphyrin and silver colloid was obtained from 4 mL of water, 1.2 mL silver colloid solution obtained from synthesis and 0.8 mL 5,10,15,20-tetrakis-(4-aminophenyl)-porphyrin-Zn(II) solution in DMSO (concentration 10^{-5} mole/L), added under stirring. The silver colloid water solution was stabilized with polyethyleneglicole (PEG).

2.2. Apparatus

UV-visible spectra were recorded on a JASCO UV- V-650 spectrometer (Japan) using standard 1 cm pass cells. Atomic force microscopy (AFM) images were performed on Nanosurf®EasyScan 2 Advanced Research AFM (Switzerland), at room temperature with samples drop-casted from THF on silica plates in noncontact mode.

3. Results and discussion

3.1. Optical and morphological characterization of silver colloid, *ZnTAPP* and *ZnTAPP-Ag-NPs* hybrid material

Fig. 2 presents the UV-vis spectrum of silver Plasmon solution (concentration 10^{-4} mole/L) having the maximum of absorption at 438 nm and the AFM images of the silver nanoparticles, that have a mix of triangular, ovoid and spherical shapes with average sizes in the range of 34 - 44 nm in diameter. Some of the spherical shaped silver particles are aggregated into dimmer structures.

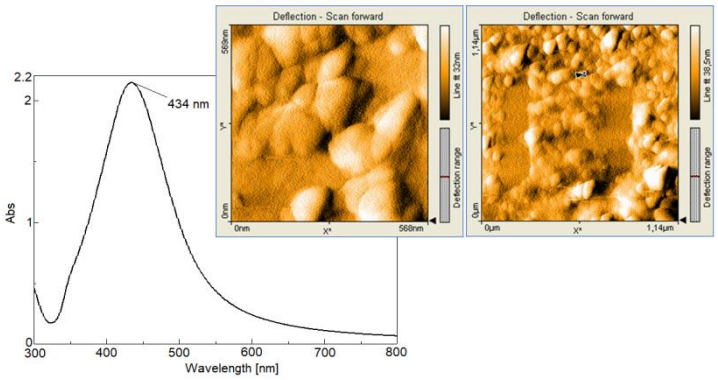

Fig. 2. The UV-vis spectrum of silver Plasmon solution and the AFM images of the silver nanoparticles.

From the overlapped UV-vis spectra of the Zn-metalloporphyrin in various solvents (Fig. 3) it can be concluded that benzonitrile, DMF and DMSO, that are polar solvents with increasing polarity in this order, are affecting the shape of the spectrum by splitting the Soret band into two distinctive peaks, a peak around 390 nm and one around 430 nm.

In the case of benzonitrile the first positioned band has a higher intensity. DMSO which is the most polar of the used solvents, provides also the most significant bathochromic effect and the best resolved Q bands, located at 566 nm and 611 nm.

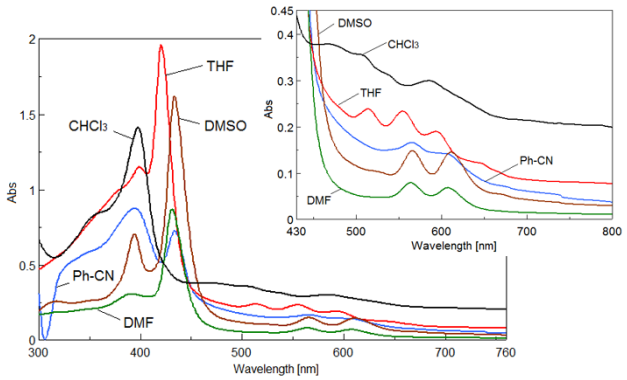

Fig. 3. Overlapped UV-vis spectra of 5,10,15,20-tetrakis-(4-aminophenyl)-porphyrin-Zn(II) solved in various solvents, at the same concentration (10^{-5}M). In detail the Q bands.

The UV-vis spectrum of the 5,10,15,20-tetrakis-(4-aminophenyl)-porphyrin-Zn(II) compound in DMSO is represented in Fig. 4, together with the corresponding AFM image. According to the AFM the Zn(II)-metalloporphyrin developed triangular arhitectures, assembled by H and J type aggregation processes into torsades with shell like shape, all oriented in the same direction. The sizes of the particles are in the range of 100 nm to 250 nm.

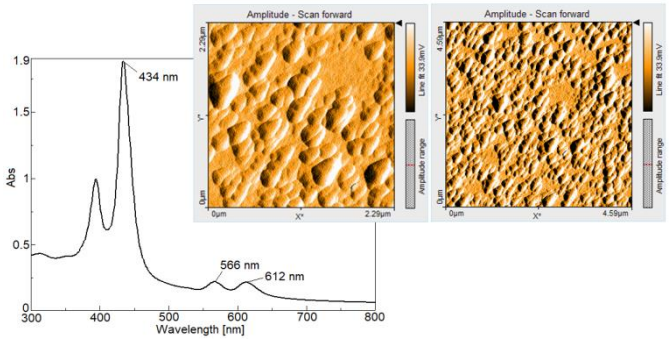

Fig. 4. The UV-vis spectrum of the 5,10,15,20-tetrakis-(4-aminophenyl)-porphyrin-Zn(II) compound in DMSO and the corresponding AFM images.

The hybrid material *ZnTAPP-AgNPs* has a different aspect in comparison with bare Zn-porphyrin. The Zn-porphyrin self-organization into triangular prisms is more precise in the case of hybrid material surface, as can be seen in Fig. 5.

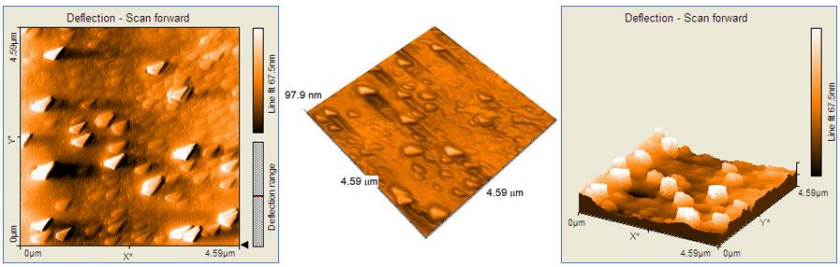

Fig. 5. The 2D and 3D AFM images of the 5,10,15,20-tetrakis-(4-aminophenyl)-porphyrin-Zn(II) -silver nanoparticles hybrid.

3.2. Detection of PAS using *ZnTAPP-AgNPs* hybrid material

The UV-vis investigation was performed by sequential adding of 0.01 mL saturated solution of PAS in water (c = 1.1 × 10^{-2} mole/L) to 6 mL of *ZnTAPP-AgNPs complex*. The absorption spectra were monitored and with increasing of PAS concentration a bathochromic shifting of the maximum of absorption from 438 nm to 460 nm took place, as can be seen in Fig. 6. This process is accompanied by the presence of one isosbestic point around 375 nm and two more located around 525 nm and 560 nm that indicate more equilibrium processes between *PAS*, *ZnTAPP* and *AgNPs*.

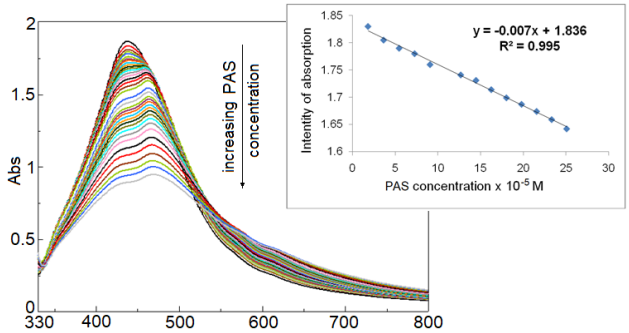

Fig. 6. Overlapped UV-vis spectra recoded after succesive adding of PAS solution to nano-Ag/Zn-porphyrin hybrid. Detail: linear dependence between the intensity of absorption registered at 438 nm and the PAS concentration.

In general, the core of Zn-porphyrin complexes is planar and is capable to axially coordinate anions, producing a distortion of the planar structure of porphyrin macrocycles. Consequently, the D_{4h} symmetry can be disturbed and the extensive delocalization of the π electrons system is perturbed. Regarding the mechanism of recognition, we presume that besides the axial coordination of *PAS* to *ZnTAPP* by its 4-amino group [20], multiple hydrogen bonds are created between NH_2-functional groups at porphyrin periphery and the two OH groups from hydroxyl and carboxyl functions of PAS.

Nevertheless, an almost perfect linear dependence between the PAS concentrations in the field of medical relevance 2-30 μg/mL (according to our graphic 0.1 – 25 x 10^{-5} mole/L of PAS) was obtained. The correlation coefficient is 0.995.

3.3. Detection of PAS using solely *ZnTAPP* in DMSO

In order to see if the generation and use of the *ZnTAPP-AgNPs* hybrid material is a must, the test were done in the same conditions as described before, but using as sensitive substance only the *ZnTAPP*. The UV-vis spectra representing the influence of increasing the concentration of the PAS on the intensity of absorbtion of Soret band (Fig. 7) gave also an excellent correlation, as can be seen in Fig. 8, but with a significant decrease in sensitivity.

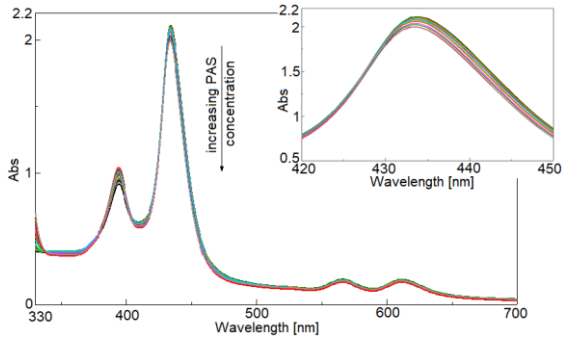

Fig. 7. Overlapped UV-vis spectra recoded after succesive adding of PAS solution to Zn-porphyrin solution in DMSO. Detail for the 434 nm region of the spectrum.

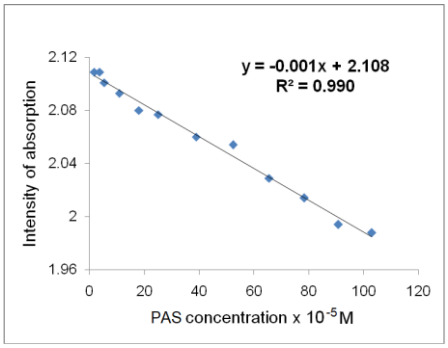

Fig. 8. Linear dependence between the intensity of absorption registered at 434 nm and the PAS concentration.

3.4. Detection of PAS using solely *AgNPs*

As it can clearly be seen in Fig. 9, the use of solely silver nanoparticles as sensing material significantly increased the sensitivity, but decreased the precision. The correlation coefficient of the dependence between PAS concentration and the intensity of absorption is of only 93.5%.

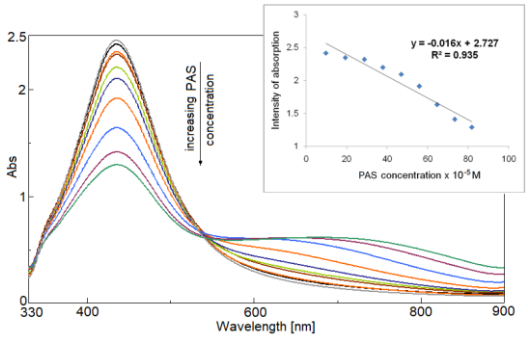

Fig. 9. Overlapped UV-vis spectra recoded after succesive adding of PAS solution to nano-Ag solution. Detail: dependence between the intensity of absorption registered at 434 nm and the PAS concentration

4. Conclusions

Para-aminosalicylic acid is still widely used for the efficient treatment of tuberculosis although it is known to cause several severe adverse side-effects.

Based on our previous experience in using silver nanoparticles and diverse porphyrin derivatives to detect biologically active or pharmaceutical compounds this work is focused on a comparison of sensing activity of PAS by simple UV-vis spectroscopy using solely *AgNPs* or *ZnTAPP* or *ZnTAPP-AgNPs* hybrid material.

The best and accurate detection results of PAS, in the medical relevance window (0.1 – 30 µg/mL) were obtained by using *ZnTAPP-AgNPs* hybrid material; the Zn-porphyrin alone offers almost the same precision but not enough sensitivity and the *AgNPs* based detection is lower regarding precision.

Based on the reported results an optical sensor based on friendly *ZnTAPP-AgNPs* hybrid material can be designed for PAS monitoring in clinical test.

Acknowledgements

This work was partially supported by the Romanian financing agency UEFISCDI – PN III No. 107 PED / 2017 / PROJECT CorOxiPor and partially by the Romanian Academy through Programme 3-Porphyrins from ICT.

This work is dedicated to the Centennial Celebration of Great Union Day of Romania (1 December 1918).

References

[1] J. Lehmann, The American Review of Respiratory Disease **909**, 53 (1964).
[2] B. Saifullah, M. Z. Hussein, S. H. Hussein-Al-Ali, P. Arulselvan, S. Fakurazi, Chemistry Central Journal 7, 72 (2013).
[3] M. M. Parvez, H. J. Shin, J. A. Jung, J.-G. Shin, Antimicrobial Agents and Chemotherapy (2017) doi:10.1128/AAC.02392-16
[4] V. Mathys, R. Wintjens, P. Lefevre, J. Bertout, A. Singhal, M. Kiass, N. Kurepina, X. M. Wang, B. Mathema, A. Baulard, B. N. Kreiswirth, P. Bifani, Antimicrobial Agents and Chemotherapy **53**(5), 2100 (2009).
[5] J. Zheng, E. J. Rubin, P. Bifani, V. Mathys, V. Lim, M. Au, J. Jang, J. Nam, T. Dick, J. R. Walker, K. Pethe, L. R. Camacho, Journal of Biological Chemistry **288**, 23447 (2013).
[6] Y. Kibleur, H. Brochart, H. S. Schaaf, A. H. Diacon, P. R. Donald, Clinical Drug Investigation (2014) DOI 10.1007/s40261-014-0172-7.

[7] M. A. Awawdeh, J. A. Legako, H. J. Harmon, Sensors and Actuators B **91**, 227 (2003).
[8] C. L. Cummins, W. M. O'Neil, E. C. Soo, D. K. Lloyd, I. W. Wainer, Journal of Chromatography B: Biomedical Sciences and Applications **697**(1-2), 283 (1997).
[9] E. Vasbinder, G. Van der Weken, Y. Vander Heyden, W. R. G. Baeyens, A. Debunne, J. P. Remon, A. M. García-Campaña**,** Biomedical Chromatography **18**, 55 (2004).
[10] M. G. H. Laghari, Y. Darwis, A. H. Memon, Tropical Journal of Pharmaceutical Research **13**(7), 1133 (2014).
[11] I. I. Miroshnichenko, G. B. Sokolova, L. V. Mokhireva, Antibiotics and Chemotherapy **54**(1-2), 20 (2009).
[12] E. S. Lianidou, P. C. Ioannou, Clinical Chemistry **42**(10), 1659 (1996).
[13] L. Hong, W. Jiang, W. Zheng, S. Zeng, Journal of Pharmaceutical and Biomedical Analysis **54**(5), 110 (2011).
[14] I. Sebarchievici, A. Lascu, G. Fagadar-Cosma, A. Palade, I. Fringu, M. Birdeanu, B. Taranu, E. Fagadar-Cosma, Comptes Rendus Chimie **21**, 327 (2018).
[15] S. Iordache, R. Cristescu, A. C. Popescu, C. E. Popescu, G. Dorcioman, I. N. Mihailescu, A. A. Ciucu, A. Balan, I. Stamatin, E. Fagadar-Cosma, D. B. Chrisey, Applied Surface Science **278**, 207 (2013).
[16] E. Fagadar-Cosma, A. Lascu, A. Palade, I. Creanga, G. Fagadar-Cosma, M. Birdeanu, Digest Journal of Nanomaterials and Biostructures **11**(2), 419 (2016).
[17] A.-M. Iordache, R. Cristescu, E. Fagadar-Cosma, A. C. Popescu, S. M. Iordache, A. A. Ciucu, A. Balan, C. Nichita, I. Stamatin, D. B. Chrisey, Comptes Rendus Chimie **21**, 270 (2018)**.**
[18] L. Bekalé, S. Barazzouk, S. Hotchandani, Particle and Particle Systems Characterization **31**, 843 (2014).
[19] I. D. Şimăndan, M. Popescu, A. Lőrinczi, A. Velea, E. Fagadar-Cosma, Digest Journal of Nanomaterials and Biostructures **5**, 1029 (2011).
[20] A. Lascu, M. Birdeanu, I. Fringu, A. Palade, A.-V. Bîrdeanu, M. Vaida, E. Fagadar-Cosma, Conference Proceedings, 9th International Conference on Nanomaterials - Research & Application, ISBN 978-80-87294-81-9, NANOCON 2017, Brno, Cseh Republic, p.410-415.
[21] I. Creangă, G. Făgădar-Cosma, A. Palade, A. Lascu, C. Enache, M. Birdeanu, E. Făgădar-Cosma, Digest Journal of Nanomaterials and Biostructures, **8**(2), 561 (2013).